연구논문

J Korean Soc Fluid Power Constr Equip Vol.11 No.3 pp.31-40 Sep. 2014
ISSN(print) 2234-8328 ISSN(online) 2287-6146
http://dx.doi.org/10.7839/ksfc.2014.11.3.031

압력커플링을 이용한 다수개의 부표를 가진 파력발전기 개발
Development of a Multi-Absorbing Wave Energy Converter using Pressure Coupling Principle

도황팅[1] · 누엔밍치[1] · 판콩빙[1] · 이세영[1] · 박형규[2] · 안경관[2*]
H. T. Do, M. T. Nguyen, C.B. Phan, S.Y. Lee, H. G. Park and K. K. Ahn

Received: 12 May. 2014, Revised: 29 May. 2014, Accepted: 20 Aug. 2014

Key Words : hydrostatic transmission, pressure coupling, wave energy converter, multi-absorbing, tilt-motion, floating buoy.

Abstract: This paper proposes a multi absorbing wave energy converter design, in which a hydrostatic transmission is used to transfer wave energy to electric energy. The most important feature of this system is its combination of the pressure coupling principle with the use of a hydraulic accumulator to eliminate the effects of wave power fluctuation; this maintains a constant speed of the hydraulic motor. Tilt motion of a floating buoy was employed as the power take-off mechanism. Furthermore, a PID controller was designed to carry out the speed control of the hydraulic motor. The design offers some advantages such as extending the life of the hydraulic components, increasing the amount of energy harvested, and stabilizing the output speed.

1. Introduction

In the recent years, wave energy is one of the most popular sources of renewable energy. There have been many studies in the field of wave energy, and there are various types of wave energy conversion systems, or wave energy converters (WECs) currently being developed, such as overtopping devices (for example, the Wave Dragon), attenuators (Pelamis) and point absorbers (WaveBob, OPT PowerBuoy), as noted in[1)]. The prior principle of WEC is that wave motion is used to create a high-pressure fluid, which is used to drive a hydraulic motor coaxially connected to an electric generator. The mechanism by which energy is transferred from waves to the WEC, and subsequently or directly into useful form, is called a hydraulic power take-off mechanism, generally known as the power take-off (PTO). The Pelamis WEC using an active control of PTO to maximize absorbed power throughout a range of sea-states was presented in[2)]. Experiments have shown that PTO efficiency reached 80%, at full-scale, over a representative range of operating conditions.

A hydraulic PTO unit has been modeled with losses to give a realistic power output and to predict PTO unit efficiency[3)], with simulation results showing that the typical hydraulic PTO unit behaves similarly to the square nature of a Coulomb damper rather than the sinusoidal nature of a viscous damper. Furthermore, the hydraulic PTO unit can be optimized by altering the motor

* Corresponding author: kkahn@ulsan.ac.kr
1 Graduate school of Mechanical and Automotive Engineering, University of Ulsan, Ulsan 680-749, Korea.
E-mail: dohoangthinh2010@gmail.com
2 School of Mechanical Engineering, University of Ulsan, Ulsan 680-749, Korea.

displacement to vary the 'effective damping' of the unit. However, only one cylinder functions as a hydraulic pump in this scheme, and thus the pressure of the fluid driving the hydraulic motor still varies over a large range. The output power is therefore not stable.

To overcome the disadvantages of the approaches above and to enhance the generated energy, we have developed a WEC called the multi-absorbing wave energy converter (MAWEC), which uses hydrostatic transmission and the pressure coupling principle. The main points of the proposed MAWEC are as follows:

- All sets of the floating buoy and cylinder are placed equidistantly to the neighboring ones by the same phase difference on the propagation route. In this way, the fluid from each cylinder can compensate for the fluid in the others, making the total flow into the accumulator nearly constant.

- The high-pressure accumulator has two functions: to smooth the fluid pressure supplied by the cylinders and to store energy. When wave conditions are strong, the wave power is more than the rated power, and the excess power is absorbed by the accumulator. When wave conditions are weak, the wave power is less than the rated power, and the accumulator compensates for the deficit in power supplied to the hydraulic motor, thereby keeping the generator velocity constant. The velocity of the hydraulic motor is controlled by a closed-loop feedback controller. Hence, the amplitude of pressure fluctuations can be reduced and the driven speed of the generator can be maintained stably even as the wave conditions change.

The remains of this paper are organized as follows: Section 2 describes the operating principle of the proposed MAWEC; Section 3 explains the mathematical model of the hydraulic system; Section 4 describes simulations and analysis of the simulation results; and Section 5 presents some conclusions.

2. Description of a Multi Absorbing Wave Energy Converter

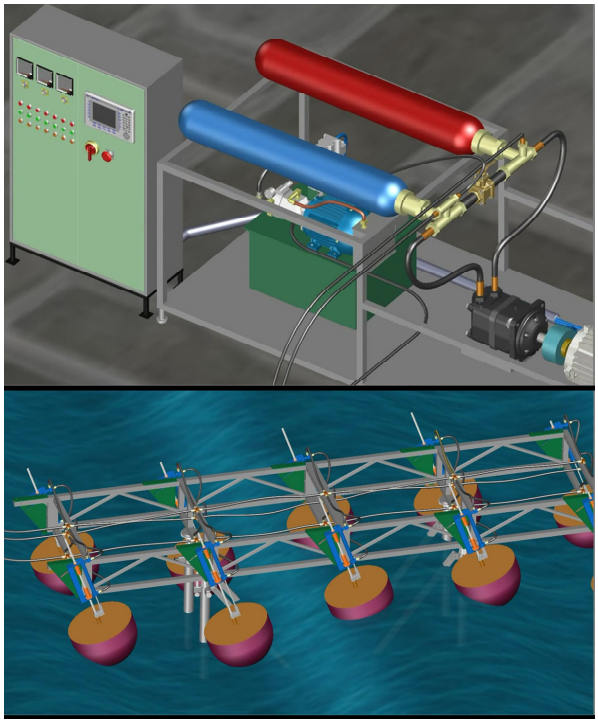

Fig. 1 3D design of MAWEC

3D design of the proposed MAWEC is given in Fig. 1. Two arrays of floating buoys are fixed to the moving shaft. One cylinder, which functions as a hydraulic pump, is attached to each shaft; one end of the cylinder is joined to the moving shaft while the other is joined to the frame. The frame and all its attached components are supported by columns, which are fixed to the sea bottom. As a sea wave arrives, the floating buoys and the moving shaft oscillate together along the tilt-longitudinal direction. The wave's force is divided into a vertical component and a horizontal component. The resultant force has the same direction as the moving direction, or differs from it by a small angle. Therefore, friction between moving parts is reduced and more power is absorbed from the wave. The piston of the cylinder moves up and down, thereby generating high-pressure fluid on both sides of the cylinder. The sliding angle of floating buoy can be adjusted by an actuator, as shown in Fig. 2.

The hydraulic circuit and control system of the proposed MAWEC are shown in Fig. 3. As mentioned above, the cylinder generates high-pressure fluid when moving up and down. When the cylinder extends, fluid from the low-pressure accumulator (LPA) fills the full bore chamber of the cylinder. Fluid in the annular chamber is pressurized and pumped to the high-pressure accumulator (HPA). Similarly, when the cylinder retracts, fluid from the LPA fills the annular chamber of the cylinder. Fluid in the full bore chamber is pressurized and pumped to the HPA. All the cylinders work on a similar principle. The check valve system only allows low-pressure fluid from the low-pressure line into the cylinder and high-pressure fluid from the cylinder into the high-pressure line to charge the HPA. In the motor control block, a PID controller was employed to control the velocity of the hydraulic motor. The driven velocity is maintained at the rated velocity by changing the swash-plate angle of the hydraulic motor to adjust the entering flow rate.

The relief valve RLV_1 releases pressure in the HPA to protect the hydraulic circuit if the operating pressure becomes too high.

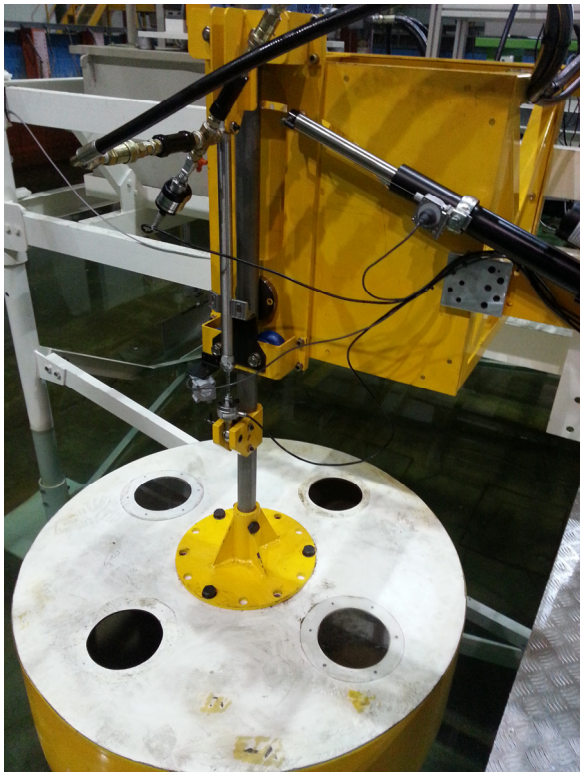

Fig. 2 Detail structure of MAWEC test rig

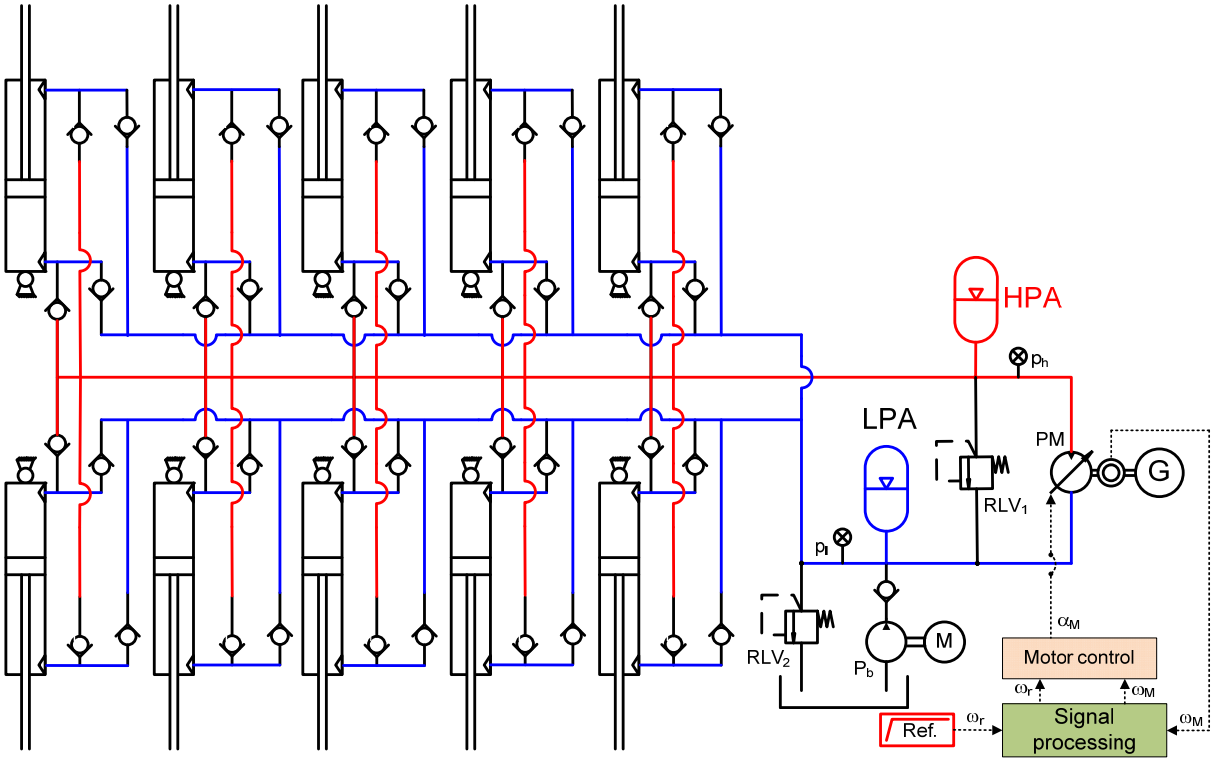

Fig. 3 Hydraulic circuit of SCHST- MPAWEC

3. Mathematical Modeling of the Multi-Absorbing Wave Energy Converter

3.1 Wave Model

An irregular ocean wave can be represented as the sum of single waves as described by the Pierson-Moskowitz spectrum 4). The irregular wave spectrum is represented by the signicant wave height H_s and the peak wave period T_p.

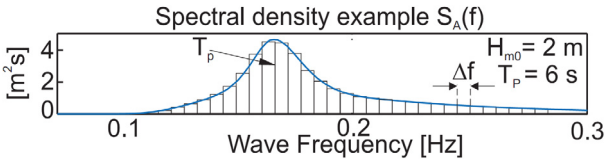

Fig. 4 Wave spectra for sea states

An irregular wave can be generated as a sum of wave components as discussed in 5):

$$Y(t)=\sum_{i=1}^{n}\sqrt{2S_A(f_i)\Delta f}\,\sin\left(2\pi f_i t+\varphi_{rand,i}\right) \tag{1}$$

where $Y(t)$ is the irregular wave displacement; $S_A(f_i)$ is the spectral density of the represented sea states; Δf is increment of wave frequency; and f_i and $\varphi_{rand,i}$ are the frequency and random phases of each component, respectively.

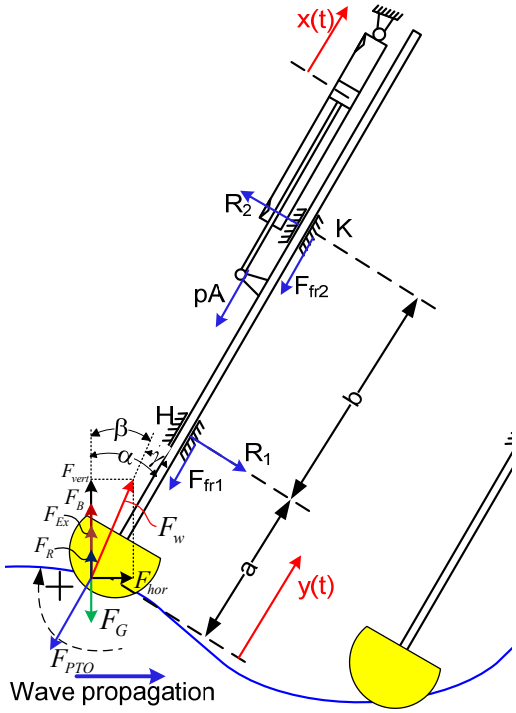

Fig. 5 Detail view and force analysis of PTOM

3.2 Hydrodynamic model of a floating buoy

The motion of a floating buoy can be described using the following equation:

$$\left(m_b+m_s\right)\ddot{y}(t)=F_w\cos\gamma-F_{PTO} \tag{2}$$

where

m_b and m_s are the mass of the floating buoy and the mass of the moving shaft, respectively, $y(t)$ is the displacement of the floating buoy, F_{PTO} is the force to move the cylinder piston to make high-pressure fluid, and F_w is the resultant force from wave on the floating buoy, included vertical component F_{vert} and horizontal component F_{hor}:

$$F_w=F_{vert}+F_{hor} \tag{3}$$

According to 6), the vertical force exerted on the floating buoy can be represented as a superposition of three components: the hydrostatics force; the excitation force applied by an incoming regular wave to a fixed float; and the radiation force experienced by an oscillating float, which is the sum of the forces created by the motion of the other buoys floating on the water. Vertical force from the wave is defined as:

$$F_{vert}=F_B+F_{Ex}+F_R-F_G \tag{4}$$

Here, F_B is the buoyant force, F_{Ex} is the excitation force and F_R is the radiation force, produced by an oscillating body creating waves on an otherwise calm sea.

The buoyant force F_B is calculated as:

$$F_B=\rho g V_s \tag{5}$$

Here, ρ is the density of water, g is the gravitational acceleration, and V_s is the volume of the floating buoy that is below the water surface, as in Fig. 6, defined as:

$$V_s=\begin{cases}\dfrac{\pi}{3}(3R-z)z^2, & 0<z\le R\\[2ex] \dfrac{2\pi}{3}R^3+\pi R^2(z-R), & R<z\le R+h\end{cases} \tag{6}$$

where, z is the submerged level of the floating buoy.

The excitation force F_{Ex} is expressed as in (3):

$$F_{EX} = \Gamma(\omega_w)\frac{H}{2}\sin\omega_w t \tag{7}$$

where $\Gamma(\omega_w)$ is the excitation force coefficient, which is dependent on the body's shape and the wave frequency(ω_w) as discussed in 5), 6), and H is the wave height (from peak to peak).

$$\Gamma(\omega_w) = \sqrt{\frac{2g^3\rho B(\omega_w)}{\omega_w^3}} \tag{8}$$

The coefficient $B(\omega_w)$ depends on the wave frequency.

The radiation force is expressed as:

$$F_R = -(m_{Ad}\ddot{y} + b_{rad}\dot{y}) \tag{9}$$

where b_{rad} is the impulse response function describing the hydrodynamic damping. The term m_{Ad} represents the "added mass"; this term is included to account for the effect that, when a float oscillates, it appears to have a greater mass due to the water that is displaced along with it, as in 4).

F_G is the gravity force, calculated as:

$$F_G = (m_b + m_s)g \tag{10}$$

Horizontal force from a wave is called as drag force, defined as:

$$F_{hor} = \frac{1}{2}\rho v^2 C_D A_{bh} \tag{11}$$

where v is the wave velocity, C_D is the drag coefficient and A_{bh} is the wet cross section of the buoy on a plane perpendicular to the direction of the wave:

$$A_{bh} = \begin{cases} R^2\left[\arcsin\left(\frac{z-R}{R}\right)\right] + \frac{\sin 2\left[\arcsin\left(\frac{z-R}{R}\right)\right]}{2} + \frac{\pi}{2}, & 0 < z \le R \\ \frac{\pi}{2}R^2 + 2R(z-R), & R < z \le R+h \end{cases} \tag{12}$$

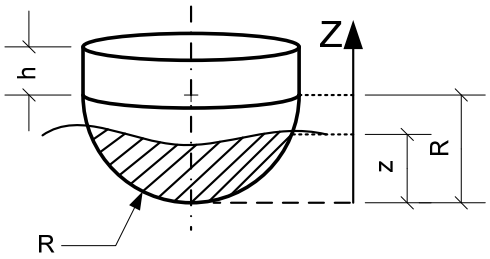

Fig. 6 Buoy shape and water level

3.3 Model of hydraulic cylinder

In this approach, cylinders were employed as hydraulic pumps to convert the kinetic energy of a floating buoy into potential energy stored in the HPA. The floating buoys are moved by waves, and then fluid in cylinders is pressurized. Define $x(t)$ as the x-coordinate of the piston. The cylinder's rod is fixed to the floating buoy, so

$$\dot{x}(t) = \dot{y}(t) \tag{13}$$

Considering the i^{th} cylinder, as in Fig. 7, the continuity equation of the bore chamber is as follows when the floating buoy moves up:

$$\frac{dp_{1i}}{dt} = \frac{\beta}{A_{p1i}(L-x_i)}\left(A_{p1i}\dot{x}_i + Q_{CVI1i} - Q_{CVO1i}\right) \tag{14}$$

and that of the annulus chamber can be expressed as follows when the floating buoy moves down:

$$\frac{dp_{2i}}{dt} = \frac{\beta}{A_{p2i}x_i}\left[A_{p2i}(-\dot{x}_i) + Q_{CVI2i} - Q_{CVO2i}\right] \tag{15}$$

Where, β is bulk modulus of oil in Pa; A_{PIi} is the piston area in m^2:

$$A_{p1i} = \pi D^2 / 4 \tag{16}$$

A_{p2i} is the rod-side area in m^2,

$$A_{p2i} = \pi(D^2 - d^2)/4 \tag{17}$$

D and d are the bore and rod diameters, respectively;

Q_{CVI1i} and Q_{CVI2i} are the input flow rates from

the LPA via check valves CVI_{1i} and CVI_{2i} to the i^{th} cylinder, respectively:

$$Q_{CVIji} = \begin{cases} C_d A_{CVIji} \sqrt{2|p_l - p_{ji}|/\rho}, & if\ p_l > p_{ji} \\ 0, & else \end{cases} \quad (18)$$

Q_{CVO1i} and Q_{CVO2i} are the output flow rates from the i^{th} cylinder via check valves CVO_{1i} and CVO_{2i} to the HPA, respectively:

$$Q_{CVOji} = \begin{cases} C_d A_{CVOji} \sqrt{2|p_{ji} - p_h|/\rho}, & if\ p_{ji} > p_h \\ 0, & else \end{cases} \quad (19)$$

i = 1, 2, …, 10 for the 1st to 10th cylinders
j = 1, for bore side of cylinders
j = 2, for annulus side of cylinders.

p_{ji} is the pressure at the cylinder ports defined by Eq. (14) and (15); p_h is the pressure of the fluid in the high-pressure line; C_d is discharge coefficient; A_{CVO1i} is the cross-section of the check valves CVO_{1i} and CVO_{2i}.

The cylinder force is calculated as:

$$F_{PTOi} = \Delta p_{ji} A_{pji} + F_{fric} \qquad j = 1,2 \quad (20)$$

Where:

$$\Delta p_{ji} = p_{ji} - p_l \quad (21)$$

p_l is considered as the pressure in the LPA.
F_{fri} is the friction of the cylinder, defined as:

$$F_{fric} = \begin{cases} |\Delta p_{1i} A_{p1i}|(1-\eta_c), & \dot{x} > 0 \\ |\Delta p_{2i} A_{p2i}|(1-\eta_c), & \dot{x} < 0 \end{cases} \quad (22)$$

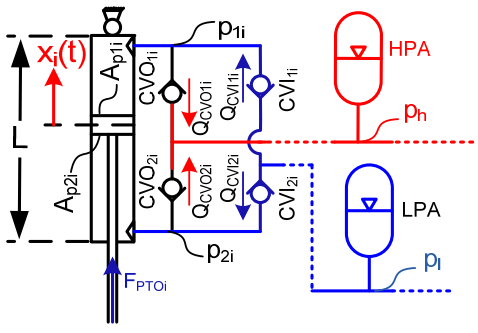

Fig. 7 Hydrodynamic of the ith cylinder

The cylinder friction F_{fric} is defined such that the cylinder has a friction coefficient η_c. The friction coefficient η_c effects to the efficiency of a cylinder.

3.4 Modeling and calculation of the HPA

In the proposed system, we employed a bladder accumulator, which was filled with nitrogen gas. According to 7), the nitrogen gas is assumed to compress and expand based on the adiabatic gas law:

$$pV^n = p_0 V_0^n = p_{\max} V_{\min}^n \quad (23)$$

Then the fluid volume in the HPA is derived as:

$$V_{HPA} = \begin{cases} 0, & if\ p_h \le p_0 \\ V_0 \left(1 - p_0 / p_h\right)^{1/n}, & else \end{cases} \quad (24)$$

where V_0 is the initial volume of the HPA, p_0 is the pre-charged pressure, p_h is the pressure at the port of the HPA and n is the adiabatic coefficient.

The energy that can be absorbed by the HPA is calculated as:

$$E = V_0 p_0^{1/n} \left[p_{\max}^{(n-1)/n} - p_0^{(n-1)/n} \right] / (n-1) \quad (25)$$

The optimal pre-charged pressure for maximum energy capacity of HPA is given by:

$$p_0 = n^{-n/(n-1)} p_{\max} \quad (26)$$

and the maximum energy stored in HPA is given by:

$$E_{\max} = p_{\max} V_0 / n^{n/(n-1)} \quad (27)$$

Then the volume of HPA can be derived as:

$$V_0 = E_{\max} n^{n/(n-1)} / p_{\max} \quad (28)$$

3.5 Model of connecting line

Using the flow continuity equation, the pressure in the high-pressure line is expressed as:

$$\frac{dp_h}{dt}=\frac{\beta}{V_h}\left(\sum_{j=1}^{2}\sum_{i=1}^{10}Q_{cvoji}-Q_{HPA}-Q_r-Q_{pm}\right) \quad (29)$$

Where:

β is the fluid bulk modulus;

V_h is the volume of the hoses;

Q_{CVOji} represents the flow rates through the check valves CVO_{1i} and CVO_{2i}, as formulated in Eq. (19);

Q_{HPA} is the flow rate into the HPA, derived based on Eq. (24) as

$$Q_{HPA}=\dot{V}_{HPA}=\begin{cases}0, \ if \ p_h\le p_0\\ \frac{1}{n}V_0\left(1-\frac{p_0}{p_h}\right)^{\frac{1-n}{n}}\frac{p_0\dot{p}_h}{p_h^2}, \ else\end{cases} \quad (30)$$

Q_r is the flow rate through the relief valve RLV_1.

According to 8), Q_r can be expressed as:

$$Q_r=\begin{cases}0, & if\ \Delta p\le p_{set}\\ C_dA_v\sqrt{2\Delta p/\rho}, & if\ \Delta p\ge p_{set}\end{cases} \quad (31)$$

Where, A_v is the valve throttling area in m^2.

Q_{pm} is the actual flow rate of the hydraulic motor as in Eq. (36), and Δp is the pressure difference between the high-pressure and low-pressure lines, which is considered to be the pressure in the LPA:

$$\Delta p=p_h-p_l \quad (32)$$

3.6 Model of the hydraulic motor

The ideal flow rate of the piston hydraulic motor is define as:

$$Q_i=\alpha D_{\max}\omega_M \quad (33)$$

where, ω is the motor rotation speed.

The volumetric efficiency, mechanical efficiency, actual flow rate and actual output torque of the piston hydraulic motor are expressed by Eq. (34-37), respectively.

$$\eta_{vM}=\alpha D_{\max}\omega_M/\left(\alpha D_{\max}\omega_M+Q_l\right) \quad (34)$$

$$\eta_{tM}=\left(\alpha_M D_{\max}\Delta p-T_{loss}\right)/\left(\alpha_M D_{\max}\Delta p\right) \quad (35)$$

$$Q_m=Q_i/\eta_{vM} \quad (36)$$

$$T_m=\alpha_M\Delta p D_{\max}\eta_{tM} \quad (37)$$

Here, Q_l and T_l are the loss flow rate and the loss torque of the pump, respectively, which were discussed in 9); $\alpha_M, D_{\max}, \Delta p$ are the displacement ratio, the maximum displacement and the pressure difference between the two ports of the motor, respectively.

4. Simulations

In the simulation, irregular wave motion was simulated as a superposition of varied sinusoidal motions. To drive the hydraulic motor tracking the reference speed, a control current I_M is sent by a PID controller, as the following equations:

$$I_M=K_pe+K_i\int edt+K_d\dot{e} \quad (38)$$

$$e=\omega_r-\omega_M \quad (39)$$

$$\alpha_M=KI_M \quad (40)$$

Where, e is the speed error of the reference speed ω_r and motor speed ω_M. The PID coefficients K_p, K_i and K_d, as shown in Table 1, were chosen by try and error method with criteria of small error, small overshoot and fast response. K is the coefficient of displacement ratio related to the control current I_M.

Table 1 PID controller

Gain	Value
Kp	70
Ki	60
Kd	40

Based on the parameters of the generator and the wave conditions, the hydraulic components of the proposed system were calculated and chosen as shown in Table 2.

Fig. 8 presents the flow rates from cylinders in/out to the HPA and to the hydraulic motor. The flow rate from the all cylinders is fluctuated, but, thanks to the effect of the HPA and the controller, the flow rate into the hydraulic motor is stable.

Fig. 9 shows the water level versus buoy displacement and the PTO force of the first floating buoy in the first 60s. PTO force is maximum positive (about 37kN) when the floating buoy moving up and PTO force is maximum negative (about 23kN) when the floating buoy moving down.

Table 2 Setting parameters of MAWEC

Components	Capacity	Unit
Floating buoy		
Diameter	4.2	m
Height	3.1	m
Mass	200	kg
Cylinder		
Piston diameter	50	mm
Rod diameter	30	mm
Length	3	m
Hyd. Motor PM		
Displacement	280	cc/rev
Max pressure	350	bar
HPA		
Volume	400	liter
Gas-pre-charge	150	bar
Max pressure	250	bar
LPA		
Volume	250	liter
Gas-pre-charge	3	bar
Check valves		
valve area	$1x10^{-4}$	m^2
Fluid		
Bulk modulus of oil	1.5	GPa
Discharge coefficient	0.7	
Generator		
Rated power	100	kW
Rated speed	1500	rpm/min
Pole number	4	poles

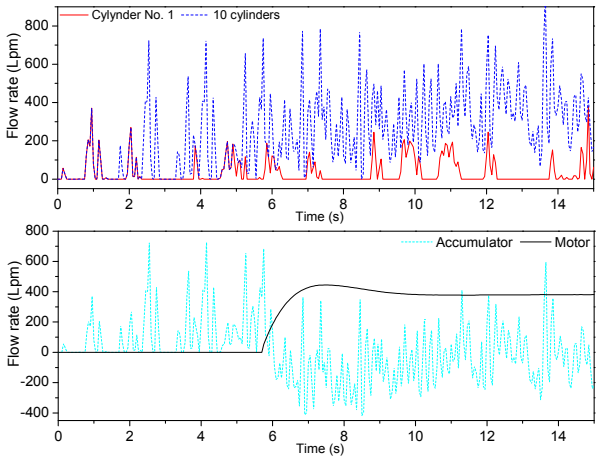

Fig. 8 The flow rates from cylinders in/out to the HPA and to the hydraulic motor

By using the HPA and the velocity controller, the flow rate into the hydraulic motor was maintained stably and the driven velocity was controlled at the rated velocity of the generator (Fig. 10).

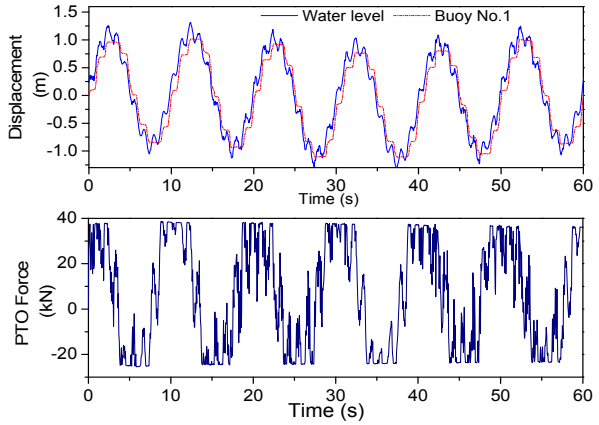

Fig. 9 The water level versus buoy displacement and PTO force

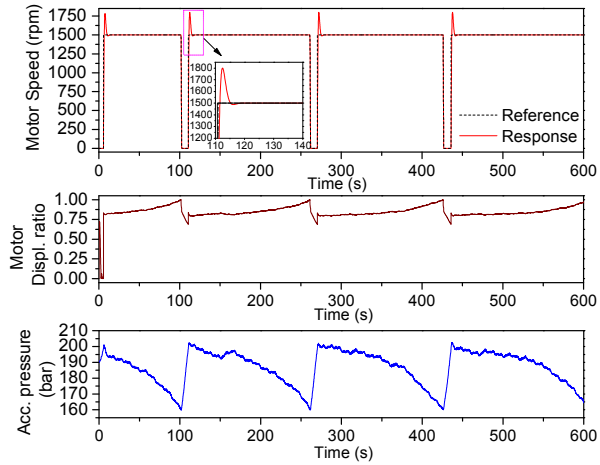

Fig. 10 Driven velocity and operating pressure

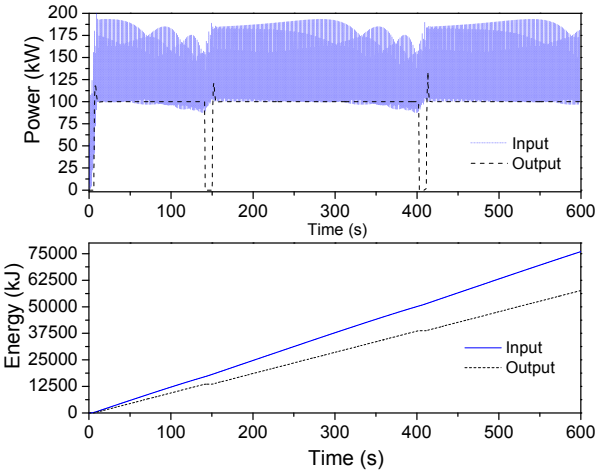

Fig. 11 Input/output powers and Input/output energies

In Fig. 10, the reference speed was defined depending on the pressure of the HPA. The reference speed was 1500 rpm if the HPA pressure was within the range of 160bar to 200bar. If the pressure of HPA was lower than 160 bar, the reference speed was switched to zero; if the pressure of HPA was higher than 200 bar, the reference speed was changed to 1500 rpm; and if the pressure was higher than 240 bar, the relief valve RLV_1 would be opened to limit the pressure to the set value and protect the system. To facilitate estimation of the efficiency of the proposed MAWEC, the wave condition was defined so that no flow would result in a pressure above the relief pressure of 240bar.

The input power fluctuated strongly, from 0 to 500 kW, but the output power was stable at 100 kW (Fig. 11). At the end of the simulation, the input and output energies were 75986kJ and 57650kJ, respectively, which corresponds to an efficiency of 75.8%.

5. Conclusions

This paper proposed a new concept called the multi-absorbing wave energy converter, which combines the use of hydrostatic transmission and the pressure coupling principle. The object of this approach is to maintain the driven speed of the generator and to reduce the effect of wave power fluctuations on the driven speed.

A mathematical model of hydraulic components was presented and simulations were carried out by using AMESim software. The simulation results indicated the effectiveness of the proposed MAWEC in maintaining the driven velocity of the generator. The efficiency of the MAWEC was 75.8% in the irregular wave condition.

In the MAWEC design simulated herein, there were five pairs of cylinders placed in two rows. However, in its actual application, more than five pairs of cylinders could be used. Each point absorber should be placed equidistantly to its neighbors by the same phase difference on the wave propagation route. In this way, the power at each point can compensate for the other absorbers, thereby reducing the amplitude of pressure fluctuations and helping to maintain the driven velocity of the generator more stably.

Acknowledgment

This work was supported by the New & Renewable Energy of the Korea Institute of Energy Technology Evaluation and Planning (KETEP) grant funded by the Korea government Ministry of Trade, Industry and Energy (G031518511).

References

1) Nielsen G, Andersen M, Argyriadis K, Butterfield S, Fonseca N, Kuroiwa T, Boulluec M. L, Liao S.J, Turnock S.R, Waegter J. Specialist Committee V.4: Ocean Wind and Wave Energy Utilization, 16th Int. Ship and Offshore Structures Congress, UK, 165-211, 2006.
2) Henderson R. Design, Simulation, and Testing of a Novel Hydraulic Power Take-Off System for the Pelamis Wave Energy Converter, Renewable Energy 2006; 31(2): 271-283.
3) Cargo C, Plummer A, Hillis A. and Schlotter M. Optimal design of a realistic hydraulic

power take-off in irregular waves, Centre of Power Transmission and Motion Control-University of Bath, 2011.
4) Hansen R. H, Andersen T. O. and Pedersen H. C. Model based design of efficient power take-off systems for wave energy converters, 12th Scandinavian International Conf. on Fluid Power, Finland, 2011.
5) Ketabdari M.J. and Ranginkaman A. Simulation of Random Irregular Sea Waves for Numerical and Physical Models Using Digital Filters. Transaction B: Mechanical Engineering 2009; 16 (3): 240-247.
6) Falnes J. Ocean Waves and Oscillating Systems. Cambridge, UK: Cambridge University Press, 2002.
7) Rabie M. G. Fluid Power Engineering, McGraw-Hill, 2009.
8) Pinches M. J. and Ashby J. G. Power Hydraulics, Englewood Cliffs, NJ: Prentice-Hall, 1988.
9) Ho T. H, Ahn K.K. Modeling and simulation of a hydrostatic transmission system with energy recuperation using a hydraulic accumulator, JMST 2010, 24 (5): 1163-1175.
10) Cummins W.E. The Impulse Response Function and Ship Motions, Schiffstechnik 1962; 9 (1661): 101-109.
11) Jen Y.M and Lee C.B. Influence of an accumulator on the performance of a hydrostatic drive with control of the secondary unit, IMechME 1993; 207: 173-184.
12) Alsina J.M. and Baldock T.E. Improved representation of breaking wave energy dissipation in parametric wave transformation models, Coastal Engineering 2007; 54 (10): 765-769.